Eur. J. Mech. B/Fluids, **18**, (1), 13-34, 1999

Large-scale instability of a fine-grained turbulent jet

Kang Ping CHEN [a]*, D.G. CRIGHTON [b]

ABSTRACT. – The initial growth of a large scale perturbation on a fine-grained turbulent jet is studied via linear stability analysis. The turbulent jet is assumed to be homogeneous and isotropic with zero mean shear, and the inviscid stream outside the jet has a uniform velocity profile. The incremental Reynolds stress caused by the large scale perturbation is modeled by a viscoelastic constitutive equation, following the analysis of Crow (1968). It is found that the jet is always unstable to both sinuous and varicose types of perturbation, with the sinuous mode having a larger growth rate. In particular, short waves are always amplified, in contrast to the short wave stabilization at low speed found by Townsend (1966) for a purely elastic jet. The growth rates of these short waves are finite, and are smaller than those for the classical Kelvin-Helmholtz instability of an inviscid jet, but larger than those for the Hooper-Boyd (1983) instability of a viscous jet with continuous velocity profile. © Elsevier, Paris.

1. Introduction

It has long been well known that certain turbulent shear flow phenomena can be explained, at least qualitatively, if the Reynolds stress increment in response to a large scale deformation is related to the rate of deformation by a viscoelastic constitutive equation (Rivlin, 1957; Liepmann, 1961; Moffatt, 1965, 1967; Townsend, 1966; Crow, 1968; Lumley, 1970; Saffman, 1977; She *et al.*, 1985; Frisch *et al.*, 1986; Kassinos and Reynolds, 1994; Speziale and Xu, 1995). A careful examination by Crow (1968) shows that this viscoelastic analogy requires that the turbulence be fine-grained and the large scale field be very weak. A rigorous derivation of a viscoelastic law for the incremental Reynolds stress was carried out by Crow for fine-grained turbulence which is homogeneous, isotropic and stationary in the absence of a mean field. Such a fine-grained turbulence could be maintained against molecular dissipation by random body forces, for example. Although highly idealized, this example does demonstrate how a viscoelastic law emerges for the Reynolds stress increment. Lumley (1970) also showed that turbulence undergoing a homogeneous deformation behaves like a classical nonlinear non-Newtonian medium.

In an effort to study the mechanism of entrainment in a turbulent jet flow, Townsend (1966) found it useful to regard the turbulent jet as an elastic medium. With the alternate assumptions of purely elastic and purely viscous jet flow, he was able, through a linear stability analysis, to provide a qualitative explanation of the growth-decay cycle, as well as of the shape of the indentations of the bounding surface that separates the turbulent and non-turbulent fluids. Townsend further provided experimental observations to support his hypothesis of an elastic jet.

In this paper, we revisit the jet problem studied by Townsend, using instead a viscoelastic constitutive law for the incremental Reynolds stress. We assume that the turbulent jet moves with a constant mean velocity with zero mean shear except at thin vortex sheet boundaries, and that the turbulence is homogeneous and isotropic. The turbulence is maintained by the agency maintaining the jet flow itself, while the perturbations are caused by means such as external acoustic forcing. These are the assumptions used in Crow's derivations, and allow us to use a viscoelastic model without ambiguity. The non-turbulent fluid outside the jet is assumed to be inviscid, and as a first step, the entrainment of such inviscid fluid into the turbulent jet is neglected. Inclusion of the

* Correspondence and reprints.
[a] Department of Mechanical and Aerospace Engineering, Arizona State University, Tempe, AZ 85287-6106, U.S.A.
[b] Department of Applied Mathematics, Theoretical Physics, University of Cambridge, Silver Street, Cambridge CB3 9EW, U.K.

entrainment complicates the conditions at the turbulent-non-turbulent interface, but in principle the problem can then still be solved similarly (*see* Reynolds (1972) for a discussion of the corresponding wake problem). Neglecting the entrainment allows us to treat the interface between the turbulent and the non-turbulent fluids as a material surface. We then perform a linear stability analysis parallel to Townsend's. The dispersion relation can be obtained analytically because of the absence of mean shear in the base state. The flow is found unstable to both sinuous and varicose types of perturbation. These instabilities are the viscoelastic generalizations of the classical Kelvin-Helmholtz (vortex sheet) instability. When viscosity or elasticity is included, the growth rate for short waves is always smaller than that of the Kelvin-Helmholtz instability for an inviscid jet, but larger than that of the Hooper-Boyd (1983) instability of a viscous jet with continuous velocity profiles. Nevertheless, the flow remains unstable to infinitely short waves, though with no more than finite growth rates. This short wave instability is due to the velocity discontinuity across the interface in the base state, as in the Kelvin-Helmholtz instability.

The results presented in this paper can also be applied to a non-turbulent, but non-Newtonian fluid jet modeled by an Oldroyd-B constitutive law with a uniform velocity profile. Thus, the type of instability discussed here may have further implications in the break-up and drop formation of a viscoelastic jet, and for such problems the short-scale behavior predicted here may indeed be significant.

Since this work was completed, the paper by Rallison and Hinch (1995) has appeared. In that paper the base jet flow is taken to have a parabolic profile, and the constitutive law is taken to be that of a purely elastic fluid, without relaxation. Thus, there is essentially no overlap with the study of the present paper.

2. A constitutive equation for the *incremental* Reynolds stress of fine-grained turbulence

The mean field equations (*i.e.*, the equations for a large scale deformation) for an incompressible turbulent flow are (Crow 1968)

$$\nabla \cdot \mathbf{U} = 0, \tag{2.1}$$

$$\rho \frac{D\mathbf{U}}{Dt} = \rho \mathbf{f} - \nabla P + \mu \nabla^2 \mathbf{U} + \nabla \cdot \tau, \tag{2.2}$$

where the substantive derivative represents convection with the mean field only, $\dfrac{D}{Dt} = \dfrac{\partial}{\partial t} + (\mathbf{U} \cdot \nabla)$, ρ, μ are the fluid density and molecular viscosity respectively, $\mathbf{f}$ is the body force per unit mass and τ is the Reynolds stress tensor defined by

$$\tau_{ij} = \frac{2}{3} T \delta_{ij} - \langle \rho u_i u_j \rangle, \tag{2.3}$$

where the bracket $\langle\ \rangle$ represents ensemble average, and T is the turbulent energy density $\rho\langle \mathbf{u}^2 \rangle/2$ (in the absence of a mean field, T is a constant in space and time).

The transport equation for the Reynolds stress tensor τ can be written (Crow 1968) as

$$\begin{aligned} \frac{D\tau}{Dt} = {} & \frac{2}{3} T(\mathbf{L} + \mathbf{L}^T) + \langle \nabla p^A \mathbf{u} + \mathbf{u} \nabla p^A \rangle - (\mathbf{L}\tau + \tau \mathbf{L}^T) \\ & + \langle \text{triple-interaction} \rangle + \langle \text{viscous} \rangle + \langle \text{body-force} \rangle, \end{aligned} \tag{2.4}$$

where $\mathbf{L} = \nabla \mathbf{U}$ is the gradient of the mean (*i.e.* large scale field) velocity, and p^A is the part of the fluctuation pressure due to the interaction between the mean and the turbulent field; it satisfies the equation

$$\nabla^2 p^A = -2\rho \mathbf{L} (\nabla \mathbf{U})^T. \tag{2.5}$$

The last three terms in (2.4), which were only written symbolically, represent stress relaxation by nonlinear scrambling, by viscous diffusion, and by body-force agitation, respectively.

Consider a large scale perturbation to incompressible, fine-grained, homogeneous, isotropic turbulence resting in statistical equilibrium with zero mean velocity. The turbulence is maintained by random body forces and has a constant energy density T. The Reynolds stress defined by equation (2.3) is then the incremental or perturbation Reynolds stress caused by the large scale perturbation. Crow (1968) showed that during the initial stage of the deformation,

$$\langle \nabla p^A \mathbf{u} + \mathbf{u} \nabla p^A \rangle = -\frac{2}{5} T(\mathbf{L} + \mathbf{L}^T). \tag{2.6}$$

Thus, for incompressible, fine-grained, homogeneous and isotropic turbulence, the equation for the incremental Reynolds stress τ becomes

$$\frac{D\tau}{Dt} = \frac{4}{15} T(\mathbf{L} + \mathbf{L}^T) - (\mathbf{L}\tau + \tau \mathbf{L}^T) + \langle \text{triple-interaction} \rangle + \langle \text{viscous} \rangle + \langle \text{body-force} \rangle, \tag{2.7}$$

valid for the initial development of the large scale perturbation. Crow showed that the Reynolds stress increment determined from equation (2.7) possesses typical viscoelastic properties, and he further proposed an integral viscoelastic constitutive equation for the incremental Reynolds stress based on the above equation. A memory function is introduced in Crow's integral equation and this memory function can be determined from the background turbulence when the mean perturbation is weak. Crow then discussed some simplified forms of his constitutive equation for the Reynolds stress increment for various limiting values of the product of a (perturbation) mean field frequency and a turbulent relaxation time. Here we propose an alternative viscoelastic constitutive equation for the incremental Reynolds stress which includes all the limiting cases of Crow, but is of rate form and as such is easier to manipulate.

We first note that equation (2.7) for the incremental Reynolds stress can be written as

$$\frac{D\tau}{Dt} + (\mathbf{L}\tau + \tau \mathbf{L}^T) = \frac{4}{15} T(\mathbf{L} + \mathbf{L}^T) + \langle \text{triple-interaction} \rangle + \langle \text{viscous} \rangle + \langle \text{body-force} \rangle, \tag{2.8}$$

The main effect of the three symbolic terms on the right hand side of (2.8) is to introduce Reynolds stress relaxation, as discussed by Crow. From the similarity of the above equation to the well known single mode convected Maxwell constitutive equation for a viscoelastic fluid (*see*, e.g., Joseph 1990), we can model these symbolic terms by introducing an integral Reynolds stress relaxation time θ_1 (Crow, 1968), and re-writing equation (2.8) in a form similar to the convected Maxwell equation

$$\theta_1 \left(\frac{D\tau}{Dt} + \mathbf{L}\tau + \tau \mathbf{L}^T \right) + \tau = 2\mu_e \mathbf{D}, \tag{2.9}$$

where $\mu_e = \frac{4}{15} \theta_1 T$ is the turbulent eddy viscosity, and $\mathbf{D}$ is the rate of strain tensor for the (perturbation) mean field,

$$\mathbf{D} = \frac{1}{2}(\mathbf{L} + \mathbf{L}^T). \tag{2.10}$$

The closure equation (2.9) is valid for the initial growth of the large scale perturbation and it can be obtained from Crow's integral equation by approximating the memory function by an exponentially decaying function with a single relaxation time. The constitutive equation (2.9) is very similar to a model equation used by

Lumley (1970) (combining his equations (4.1), (4.2) and (4.3)) for turbulence under homogeneous deformations. The deformation considered here, however, could be arbitrary, as in Crow (1968). The turbulent relaxation time θ_1 is a property of the isotropic turbulence itself, and an expression for this relaxation time can be given in terms of the wavenumber-frequency spectrum of the background isotropic turbulence E (Crow, 1968):

$$\theta_1 = \int_0^\infty \int_0^\infty \frac{E(k,\omega)}{T} = \frac{2\nu k^2)^3}{[\omega^2 + (\nu k^2)^2]^2} dk\, d\omega, \tag{2.11}$$

where ν is the kinematic viscosity of the fluid, and k and ω are the wavenumber and frequency, respectively.

The incremental Reynolds stress satisfying the constitutive equation (2.9) exhibits typical viscoelastic behavior. Both the normal Reynolds stress difference (Reynolds stress anisotropy) in simple shear flows and the Reynolds stress relaxation phenomena described by Crow are included in this model. For simple shear flows, a negative normal (Reynolds) stress difference is predicted from equation (2.9) (so that, say, $\langle \rho u_1^2 \rangle$ is necessarily positive). The negative normal Reynolds stress difference creates an equivalent compression along the streamlines of the mean field in simple shear flows. In this regard, we can think of the fine-grained, isotropic turbulence as a viscoelastic medium with a negative normal stress difference in simple shear flows. Since no second normal stress difference (cross-stream normal stress) is predicted from (2.9), this equation cannot be used to account for the secondary motions observed in some turbulent flows (e.g. in non-circular ducts) which is caused by the second normal (Reynolds) stress difference.

Crow's derivation, and thus the proposed equation (2.9), is rigorously valid for the initial development of the large scale perturbation when the background turbulence is homogeneous and isotropic. Equation (2.9) is used in this paper to study the implications of viscoelastic-like models to the initiation of the large scale motions on a fine-grained turbulent jet.

3. Governing equations for the linear stability of a fine-grained turbulent jet

Consider a large scale perturbation to the motion of an incompressible, fine-grained isotropic turbulent jet with a zero mean velocity, as shown in Figure 1. The turbulence is maintained by random body force agitation and the perturbations are caused by external forcing. The problem is formulated in a frame of reference moving with the jet. The whole problem is two-dimensional, but relations such as $\mu_e = \frac{4}{15}\theta_1 T$, derived for three-dimensional fine-grained turbulence, will be assumed to hold in the characterization of the turbulence. The non-turbulent fluid outside the jet is inviscid and moves in the negative x direction with a uniform velocity U_0. The shear layer between the turbulent jet and the surrounding inviscid stream is modeled as a discontinuity so that the large scale perturbations considered have length scales much larger than the shear layer thickness and the small scales of the fine-grained turbulence. Since the basic state has no shear, equation (2.9) is reduced to a linear viscoelasticity equation when linearized. Then the linearized perturbation equations for the mean perturbation fields are:

$$\nabla \cdot \mathbf{U} = 0, \tag{3.1}$$

$$\rho \frac{\partial \mathbf{U}}{\partial t} = -\nabla P + \nabla \cdot \mathbf{S}, \tag{3.2}$$

$$\mathbf{S} = 2\mu \mathbf{D} + \tau, \tag{3.3}$$

$$\tau + \theta_1 \frac{\partial \tau}{\partial t} = 2\mu_2 \mathbf{D}. \tag{3.4}$$

Equations (3.3) and (3.4) can be combined into a single equation for $\mathbf{S}$:

$$\mathbf{S} + \theta_1 \frac{\partial \mathbf{S}}{\partial t} = 2\eta \left(\mathbf{D} + \theta_2 \frac{\partial \mathbf{D}}{\partial t} \right), \tag{3.5}$$

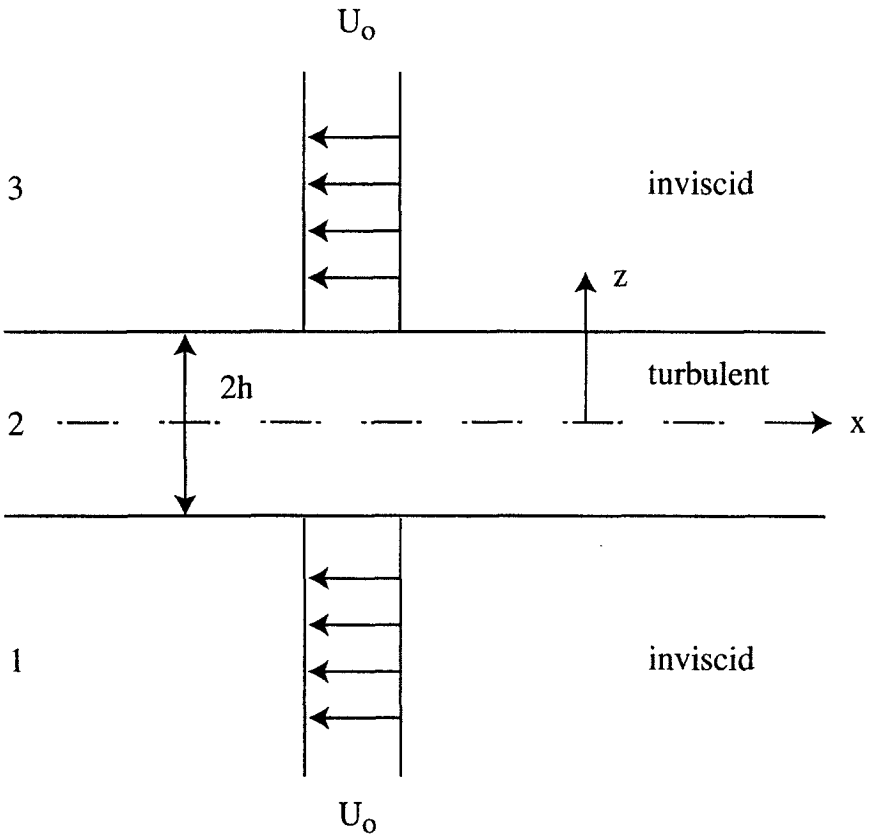

Fig. 1. – Flow configuration in the frame of reference moving with the jet.

where $\eta = \mu + \mu_2$ is the effective viscosity of the turbulent jet, and $\theta_2 = (\mu/\eta)\theta_1$ is a strain relaxation time (or retardation time). For turbulent flows, $\varepsilon = \mu/\eta$ is usually small, and thus $\theta_2 = \varepsilon\theta_1$ is small.

We choose half of the jet width h as the length scale, U_0 as the velocity scale, and h/U_0 as the time scale. Stresses in the jet are scaled with $\eta U_0/h$, and the pressures in both the jet and the surroundings are scaled with ρU_0^2. The dimensionless groups arising from this non-dimensionlization are the Reynolds number,

$$\mathrm{Re} = \frac{\rho U_0 h}{\eta}, \tag{3.6}$$

defined in terms of the effective viscosity (this is typically about 25 for a plane jet; *see* Tennekes and Lumley, 1972), and the turbulent Weissenberg number,

$$Wi = \frac{\theta_1 U_0}{h}. \tag{3.7}$$

The dimensionless linearized equations for the disturbances are:

in the jet, $-1 \leq z \leq 1$:

$$\nabla \cdot \mathbf{U} = 0, \tag{3.8}$$

$$\frac{\partial \mathbf{U}}{\partial t} = -\nabla P + \frac{1}{\mathrm{Re}} \nabla \cdot \mathbf{S}, \tag{3.9}$$

$$\mathbf{S} + Wi \frac{\partial \mathbf{S}}{\partial t} = 2\left(\mathbf{D} + \varepsilon Wi \frac{\partial \mathbf{D}}{\partial t}\right), \tag{3.10}$$

and in the inviscid surroundings, regions 1 and 3:

$$\nabla \cdot \mathbf{U} = 0, \tag{3.11}$$

$$\frac{\partial \mathbf{U}}{\partial t} - \frac{\partial \mathbf{U}}{\partial x} = -\nabla P. \tag{3.12}$$

The interface conditions are:
at $z = -1$ (the lower interface is perturbed to $-1 + \xi(x,t)$):

$$w_1 = \frac{\partial \xi}{\partial t} - \frac{\partial \xi}{\partial x}, \tag{3.13}$$

$$w_2 = \frac{\partial \xi}{\partial t}, \tag{3.14}$$

$$(S_{xz})_2 = 0, \tag{3.15}$$

$$-p_2 + \frac{(S_{zz})_2}{\mathrm{Re}} + p_1 = 0; \tag{3.16}$$

at $z = 1$ (the upper interface is perturbed to $1 + \delta(x,t)$):

$$w_3 = \frac{\partial \delta}{\partial t} - \frac{\partial \delta}{\partial x}, \tag{3.17}$$

$$w_2 = \frac{\partial \delta}{\partial t}, \tag{3.18}$$

$$(S_{xz})_2 = 0, \tag{3.19}$$

$$-p_2 + \frac{(S_{zz})_2}{\mathrm{Re}} + p_3 = 0. \tag{3.20}$$

It can be shown that Squire's transformation exists for the model equations used here, although no theorem can be proven for the problem under consideration (Yiu and Chen 1994, unpublished note. For problems without free surfaces, *see* Azaiez and Homsy 1994). Thus it is sufficient to consider two-dimensional disturbances. The normal mode equations can be obtained by decomposing the disturbances into normal modes with a multiplier $\exp[i\alpha(x - ct)]$, where α is the stream-wise wavenumber and c is the complex wave speed (only temporal modes are considered in this study). In the jet, (3.10) gives

$$\mathbf{S} = 2Q\mathbf{D}, \tag{3.21}$$

where

$$Q = \frac{1 - \varepsilon i\alpha cWi}{1 - i\alpha cWi} \tag{3.22}$$

can be considered as a complex viscosity. After eliminating S we have

$$i\alpha u_2 + w_2' = 0, \tag{3.23}$$

$$-i\alpha c u_2 = -i\alpha p_2 + \frac{Q}{\mathrm{Re}}(-2\alpha^2 u_2 + u_2'' + i\alpha w_2'), \tag{3.24}$$

$$-i\alpha c w_2 = -p_2' + \frac{Q}{\mathrm{Re}}[i\alpha(u_2' + i\alpha w_2) + 2w_2''], \tag{3.25}$$

where a prime stands for the derivative with respect to z. In the inviscid regions we have

$$i\alpha u_i + w_i' = 0, \tag{3.26}$$

$$i\alpha(1+c)u_i = i\alpha p_i, \tag{3.27}$$

$$i\alpha(1+c)w_i = p_i', \tag{3.28}$$

for $i = 1, 3$. The interface conditions are readily written in normal mode form.

4. The dispersion relation

The eigenvalue problem presented in the above section can be further simplified to a fourth order ordinary differential equation for w_2 with four boundary conditions:

$$\left(D^2 - \alpha^2 + \frac{i\alpha c\mathrm{Re}}{Q}\right)(D^2 - \alpha^2)w_2 = 0, \tag{4.1}$$

with, at $z = -1$,

$$w_2''' + \alpha^2 w_2 = 0, \tag{4.2}$$

$$cQ(w_2'' - 3\alpha^2 w_2') + i\alpha c^2 \mathrm{Re} w_2' - i\alpha^2 \mathrm{Re}(1+c)^2 w_2 = 0; \tag{4.3}$$

and at $z = 1$,

$$w_2'' + \alpha^2 w_2 = 0, \tag{4.4}$$

$$cQ(w_2'' - 3\alpha^2 w_2') + i\alpha c^2 \mathrm{Re} w_2' + i\alpha^2 \mathrm{Re}(1+c)^2 w_2 = 0, \tag{4.5}$$

where $D = \dfrac{d}{dz}$. The general solution to equation (4.1) is

$$w_2 = A_1 \sinh \alpha z + A_2 \cosh \alpha z + A_3 \sinh \beta z + A_4 \cosh \beta z, \tag{4.6}$$

where

$$\beta = \left(\alpha^2 - \frac{i\alpha c\mathrm{Re}}{Q}\right)^{1/2}, \tag{4.7}$$

and the dispersion relation is found to be

$$p_1 \tanh\alpha \tanh^2\beta + p_2 \tanh^2\alpha \tanh\beta + p_3 \tanh\alpha \tanh\beta + p_4 \tanh^2\alpha + p_5 \tanh^2\beta + p_6 \tanh\alpha + p_7 \tanh\beta = 0, \tag{4.8}$$

where the coefficients p_1 to p_7 are functions of β and are listed in the Appendix. The dispersion function on the left of (4.8) is an odd function of the parameter β so either branch for β will do, and for definiteness we keep the real part of β non-negative, $RE(\beta) \geq 0$, in all the calculations.

The dispersion relation (4.8) is very complicated. Two independent fundamental cases are the sinuous mode and the varicose mode, which represent anti-symmetric and symmetric disturbances respectively. These two modes are easier to analyze and indeed provide, in linear combination, the general solution.

4.1. The anti-symmetric (sinuous) mode

For the sinuous mode, the eigenfunction is even in z, $w_2(-z) = w_2(z)$. Thus the eigenfunction has the form

$$w_2 = A_2 \cosh \alpha z + A_4 \cosh \beta z, \tag{4.9}$$

with dispersion relation

$$\mathrm{Re}^2(1-i\alpha cWi)^2(1+c)^2-[2\alpha-ic\mathrm{Re}(1-i\alpha cWi)-\varepsilon 2i\alpha^2 cWi]^2 \tanh\alpha+4\alpha\beta(1-\varepsilon i\alpha cWi)^2 \tanh\beta = 0. \tag{4.10}$$

4.2. The symmetric (varicose) mode

For the varicose mode, the eigenfunction is odd in z, $w_2(-z) = -w_2(z)$. Thus the eigenfunction has the form

$$w_2 = A_1 \sinh \alpha z + A_3 \sinh \beta z, \tag{4.11}$$

with dispersion relation

$$4\alpha\beta(1-\varepsilon i\alpha cWi)^2 \tanh\alpha+[(2i\alpha+c\mathrm{Re}-i\alpha c^2\mathrm{Re}Wi+\varepsilon 2\alpha^2 cWi)^2+\mathrm{Re}^2(1+c)^2(i-i\alpha cWi)^2 \tanh\alpha] \tanh\beta=0. \tag{4.12}$$

We can eliminate the Weissenberg number Wi by setting

$$Wi = E\mathrm{Re}, \tag{4.13}$$

where

$$E = \frac{\theta_1 \eta}{\rho h^2} \tag{4.14}$$

is the elasticity number which depends on the fluid properties and the flow geometry, but not on the flow field. It depends also on the turbulent energy density T and the turbulence relaxation time θ_1.

In the following, we will study the sinuous mode in some detail. It will be shown later, in section 8, that the growth rate of the varicose mode is no greater than that of the sinuous mode.

5. Asymptotic analysis of the sinuous mode I: $\varepsilon = 0$

When one neglects the molecular viscosity, $\varepsilon = 0$, (4.10) reduces to

$$\mathrm{Re}^2(1 - i\alpha cWi)^2(1 + c)^2 - [2\alpha - ic\mathrm{Re}(1 - i\alpha cWi)]^2 \tanh\alpha + 4\alpha\beta \tanh\beta = 0. \tag{5.1}$$

An exact solution of (5.1) is

$$c = -\frac{i}{\alpha Wi} = -\frac{i}{\alpha E\mathrm{Re}}, \tag{5.2}$$

which represents stable modes.

5.1. The long waves

In the long wave limit, $\alpha \to 0$, the asymptotic solution for c is given by

$$c = -1 \pm i\alpha^{1/2} + \alpha \pm i\alpha^{3/2} + O(\alpha^2). \tag{5.3}$$

This asymptotic solution is valid for both viscous and viscoelastic jets, provided the Reynolds number and the elasticity number are both of order one. It shows that the sinuous mode is always unstable to long wave disturbances, and it has a wave speed equal to $-1 + \alpha$, and a growth rate $\alpha^{3/2}(1 + \alpha)$. Thus, the long sinuous instability wave is essentially stationary if viewed from a fixed (laboratory) reference frame.

5.2. The short waves

The "short waves" considered in this study are the waves with wavelengths much shorter compared to the jet width h, but much larger than the shear layer thickness and the small scales of the turbulence. The behavior of the sinuous mode in the short wave limit, $\alpha \to \infty$, is more complicated, and it depends strongly on the elastic properties. When $\alpha \to \infty$, the dispersion relation (5.1) is reduced to

$$\mathrm{Re}^2(1 - i\alpha cWi)^2(1 + c)^2 - [2\alpha - ic\mathrm{Re}(1 - i\alpha cWi)]^2 + 4\alpha\beta = 0, \tag{5.4}$$

under the restriction that the real part of β is non-negative, $RE(\beta) \geq 0$.

For comparison purpose, we shall discuss the purely viscous case and the viscoelastic case separately.

5.2.1. *The purely viscous jet*

For a purely viscous jet, $Wi = 0$, we obtain

$$c = i\frac{\mathrm{Re}}{2\alpha} + O\left(\frac{1}{\alpha^2}\right). \tag{5.5}$$

Therefore, to leading order the sinuous mode has a wave speed

$$c_r = 0, \tag{5.6}$$

and a bounded growth rate

$$\sigma = \alpha IM(c) = \frac{\mathrm{Re}}{2}. \tag{5.7}$$

This is in contrast to the classical Kelvin-Helmholtz instability of an inviscid jet, which gives an unbounded growth rate, proportional to the wave number α , for short waves. The growth rate (5.7) is larger than that of the Hooper-Boyd instability for a viscous jet with continuous velocity profile, which gives an infinitely small growth rate (Hooper and Boyd 1983).

5.2.2. *The viscoelastic jet*

For a viscoelastic jet $E \neq 0$. If we assume the following expansion for the eigenvalue c

$$c = c_0\frac{c_1}{\alpha} + O\left(\frac{1}{\alpha^2}\right). \tag{5.8}$$

then to leading order we have

$$4 - 4c_0^2\chi + c_0^2\chi^2 + 2c_0^3\chi^2 + 2c_0^4\chi^2 - 4(1 - c_0^2\chi)^{1/2} = 0, \tag{5.9}$$

where

$$\chi = E\mathrm{Re}^2. \tag{5.10}$$

This leading order equation for the short waves is exactly the same as equation (A20) of Townsend (1966) for a jet of elastic jelly. The rigidity of the jet, n, corresponds to $1/\chi$. A double root of (5.9) is always $c_0 = 0$.

In the limit of slow flows, $\chi \to 0$, equation (5.9) has the following roots:

$$c_0 = \begin{cases} 0, \text{ double} \\ \pm\dfrac{0.839287}{\chi^{1/2}}, \\ \dfrac{\pm 1.41964 \pm i0.606291}{\chi^{1/2}}, \end{cases} \tag{5.11}$$

However, it can be verified that corresponding to the complex conjugate roots given in equation (5.11), the condition $RE(\beta) \geq 0$ is always violated. Therefore these complex conjugate roots have to be excluded; they are not close to a root of equation (5.11). The two non-zero real roots, $c_0 = \pm\dfrac{0.839287}{\chi^{1/2}}$, are mathematically and physically acceptable neutral elastic modes.

In the limit $\chi \to \infty$, on the other hand, we recover from (5.9) the classical result of Kelvin-Helmholtz instability for an inviscid jet:

$$c_0 = -\frac{1 \pm i}{2}. \tag{5.12}$$

Comparing the two opposite limits of $\chi \to 0$ and $\chi \to \infty$, we expect that there exists a critical value χ_c such that when $\chi > \chi_c$, at least one of the neutral elastic modes becomes unstable. Numerical computation from equation (5.9) indicates that, as χ is gradually increased from zero, the two neutral elastic mode phase speeds remain real valued until

$$\chi = \chi_c = 3.2135, \tag{5.13}$$

at which they coincide with each other, and give

$$c_0 = -0.354137. \tag{5.14}$$

For $\chi > \chi_c = 3.2135$, a pair of complex conjugate roots emerges, and one of the elastic modes becomes unstable with growth rate proportional to the wave number α. But this growth rate is always smaller than that of an inviscid jet (Kelvin-Helmholtz instability). For $0 < \chi < \chi_c$, one of the neutral elastic modes always has a negative wave speed, while the other one has a positive wave speed for $0 < \chi < 2$ and a negative wave speed when χ is increased past 2. We shall refer to the value of the former as c_0^-, and of the latter as c_0^+.

The next order correction c_1 can be calculated. Two possibilities need to be considered separately:

(A) $c_0 = 0$: elastic modification of the viscous mode.

For the root near $c = 0$, we find

$$c = \begin{cases} \pm\dfrac{1}{\alpha}\dfrac{i}{E\mathrm{Re}}, & \text{exact solution} \\ \dfrac{1}{\alpha}\dfrac{i\mathrm{Re}}{2 - E\mathrm{Re}^2} + O\left(\dfrac{1}{\alpha^2}\right). \end{cases} \tag{5.15}$$

The first root is the damping mode, and the second root is the modification of the viscous mode (5.5) by viscoelasticity.

It is clear that in the short wave limit elasticity increases the growth rate of the unstable viscous mode if $0 < \chi = E\mathrm{Re}^2 < 2$. If $\chi > 2$, however, elasticity stabilizes the viscous mode in the short wave limit. There is an apparent singularity at $\chi = 2$ which gives an unbounded growth rate as this limit is approached from below. The actual growth rate is finite at $\chi = 2$ and the expansion (5.8) is not uniformly valid for χ near 2. This singular behavior for a viscoelastic medium is similar to those found by Wilson (1990) for the Taylor-Saffman problem and Aitken and Wilson (1993) for the Rayleigh-Taylor problem for an upper convected Maxwell fluid ($\varepsilon = 0$). We will show later on how this singularity can be removed by including a non-zero ε.

(B) $c_0 \neq 0$: elastic modes.

In this case, we are seeking higher order corrections to the elastic modes emerging from $\pm\frac{0.839287}{\chi^{1/2}}$ as χ is increased. If $\chi > 3.2135$, one of these elastic modes is *unstable* at $O(1)$, *i.e.* c_0 appears as a pair of complex conjugates. In this case, the growth rate is ultimately proportional to the wavenumber α and so unbounded.

Consider $\chi < 3.2135$. Then c_1 is found to be given by

$$c_i = -i\frac{\mathrm{Re}}{\chi}\frac{(2 - \chi - 2c_0^2\chi - 2c_0^2\chi)\sqrt{1 - 2c_0\chi - 1}}{(4 - \chi - 3c_0\chi - 4c_0^2\chi)\sqrt{1 - 2c_0^2\chi - 2}} \tag{5.16}$$

Numerical computation of (5.16) shows that, for $c_0 = c_0^-$, we always have $IM(c_1^-) < 0$, while for $c_0 = c_0^+$ $IM(c_1^+)$ changes from negative to positive values when χ passes through 2. Thus, the elastic "+" mode becomes *unstable* with a finite growth rate when $\chi > 2$.

The short wave behavior of the sinuous mode for $\varepsilon = 0$ can be summarized as follows:

(A) Purely viscous mode:

$$c = \frac{1}{\alpha}\frac{i\mathrm{Re}}{2} + O\left(\frac{1}{\alpha^2}\right); \tag{5.17}$$

(B) Viscous mode modified by elasticity:

$$c = \frac{1}{\alpha}\frac{i\mathrm{Re}}{2 - E\mathrm{Re}^2} + O\left(\frac{1}{\alpha^2}\right); \tag{5.18}$$

(C) Elastic modes:

$$c = c_0^- + \frac{c_1^-}{\alpha} + O\left(\frac{1}{\alpha^2}\right); \qquad \text{(stable)} \tag{5.19}$$

$$c = c_0^+ + \frac{c_1^+}{\alpha} + O\left(\frac{1}{\alpha^2}\right), \qquad \text{(unstable if } \chi > 2\text{)}. \tag{5.20}$$

We conclude from the above analyses that the short waves are always *unstable*, and the maximum growth rate for $\alpha \to \infty$ is

$$\sigma_{\max} = \begin{cases} \dfrac{\mathrm{Re}}{2 - E\mathrm{Re}^2} + O\left(\dfrac{1}{\alpha}\right), & 0 < \chi < 2, \\ IM(c_1^+) + O\left(\dfrac{1}{\alpha}\right), & 2 < \chi < 3.2135, \\ \alpha IM(c_0^+) + O(1), & \chi > 3.2135. \end{cases} \tag{5.21}$$

Since it is found numerically that $IM(c_0^+) < \dfrac{1}{2}$, the maximum growth rate is always smaller than that of the Kelvin-Helmholtz instability of an inviscid jet in the short wave limit. In fact, $IM(c_0^+)$ approaches the inviscid limit $\frac{1}{2}$ monotonically with increasing χ. Since the growth rate in the short wave limit is at least of order one, the short wave instabilities are always stronger than the Hooper-Boyd instabilities for a viscous jet with continuous velocity profiles, which have arbitrarily small growth rates. Furthermore, the wave speeds here for short waves are always greater than the inviscid value of $-\frac{1}{2}$, and tend to this limit as χ approaches infinity.

6. Asymptotic analysis of the sinuous mode II $\varepsilon \neq 0$

As in the case $\varepsilon = 0$, the dispersion relation (4.10) still has the exact solution $c = -\dfrac{1}{\alpha}\dfrac{i}{E\mathrm{Re}}$ which are the damped stable modes. The molecular viscosity, although small compared to the eddy viscosity, plays an important role in the short-wave stability of the jet. In equation (3.10), the small parameter ε, which is the ratio of the molecular viscosity to the sum of the molecular and the eddy viscosities, appears as a factor multiplying the highest derivative term, $\dfrac{\partial \mathbf{D}}{\partial t}$. Accordingly, a small amount of molecular viscosity has a dramatic influence on the short wave behavior for the elastic modes. The long wave behavior of the sinuous mode, however, remains the same as in the case $\varepsilon = 0$, up to $O(\alpha^{3/2})$. The presence of molecular viscosity has no effect on such long waves.

For short waves, it is found that

$$c = \begin{cases} -\dfrac{1}{\alpha}\dfrac{i}{E\mathrm{Re}}, \text{ (exact solution)} & (6.1a) \\ i\dfrac{-(2 - E\mathrm{Re}^2) \pm \sqrt{2 - E\mathrm{Re}^2)^2 + \varepsilon 8 E\mathrm{Re}^2}}{\alpha\varepsilon 4 E\mathrm{Re}} + O\left(\dfrac{1}{\alpha^2}\right). & (6.1b) \end{cases}$$

Therefore instability persists for short waves even when $\varepsilon \neq 0$ (the "+" solution in (6.1b) is always unstable). The singular behavior of the elastically modified viscous mode (5.18) at $\chi = E\mathrm{Re}^2 = 2$ is, however, smoothed out when $\varepsilon \neq 0$. Moreover, a non-zero value of ε guarantees *bounded* growth rates as well as zero wave speeds for short waves. This reduction in the growth rate by an order of magnitude (in terms of powers of α) for non-zero ε for the short wave limit is achieved by forcing a unique value of $c_0 (= 0)$. In fact, $\varepsilon \to 0$ is a singular limit for the eigenvalue problem since ε multiplies the highest derivative term in equation (3.10), as mentioned earlier.

7. Maximum growth rates for the sinuous mode

A simple Newton iteration is used to find the eigenvalue c for an arbitrary wavenumber α from the dispersion relations (5.1) for $\varepsilon = 0$, and (4.10) for $\varepsilon \neq 0$. For a fixed set of parameters, we start the calculations for

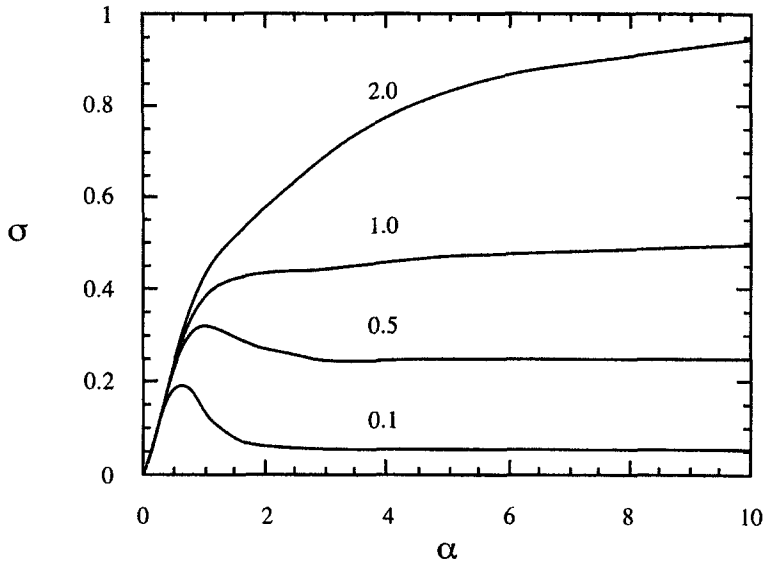

Fig. 2. – Growth rates for the sinuous mode for a purely viscous jet. Re = 0.1, 0.5, 1.0, 2.0. The numerical values above each curve indicate the corresponding Reynolds numbers.

long waves, for which good initial guesses can be provided from the long wave asymptotics, and then progress toward shorter waves. This simple strategy works well, and the calculations have been checked against results obtained from nonlinear equation solvers as well as results from MATHEMATICA. All the numerical results are in exact agreement with both the small wavenumber and the large wavenumber asymptotics.

Growth rates for a purely viscous jet are presented in Figure 2 for Re = 0.1, 0.5, 1.0, 2.0. The growth rate reaches a maximum at an order one wavenumber for small Reynolds numbers, as for Re = 0.1, 0.5. As the Reynolds number is increased to one, this growth rate maximum disappears. In fact, for any Reynolds number greater than one, the growth rate increases monotonically with the wavenumber α, and the maximum growth rate occurs in the short wave limit $\alpha \to \infty$, where it is given by the asymptotic formula

$$\sigma = \alpha IM(c) = \frac{\mathrm{Re}}{2}. \tag{7.1}$$

The wave speeds, which are plotted in Figure 3, increase with the wavenumber, and all approach zero from below as $\alpha \to \infty$. The wave speed decreases with Reynolds number.

To incorporate elastic effects, we shall first consider the case $\varepsilon = 0$. If $\chi = E\mathrm{Re}^2 < 2$, then the unstable mode is the one that modifies the viscous mode, and gives a limiting growth rate for short waves. An example of this is presented in Figure 4, where the growth rates for Re = 0.5, E = 0, 1.0, 3.0, 5.0, 8.0 are compared. As can be seen from this figure, elasticity increases the growth rate, as one might have expected from the short wave asymptotic analysis. As the elasticity parameter E is increased, the maximum in the growth rate is increased, and develops into a local maximum when the short wave limiting value exceeds this maximum (e.g. E = 3.0, 5.0). For $\chi < 2 (E < 8.0)$, the growth rate levels off to a constant $\frac{2}{8-E}$ when $\alpha \to \infty$, as determined by the short wave asymptotics. When $\chi = 2$, which corresponds to the curve for E = 8.0, the growth rate approaches infinity, as indicated by the short wave singularity for this value of χ. Elasticity reduces the wave speeds, as shown in Figure 5. As in the purely viscous case, all the wave speeds approach zero from below when $\alpha \to \infty$, including the curve for $E = 8.0 (\chi = 2)$.

Results covering $0 \leq \chi \leq 3.2135$, for Re = 1, and E = 0, 0.5, 1.0, 1.5, 2.0, 2.4, 3.0, 3.1, 3.2, 3.2135, are given in Figures 6 and 7. The purely viscous case $E = 0$ is included for comparison purposes. The growth

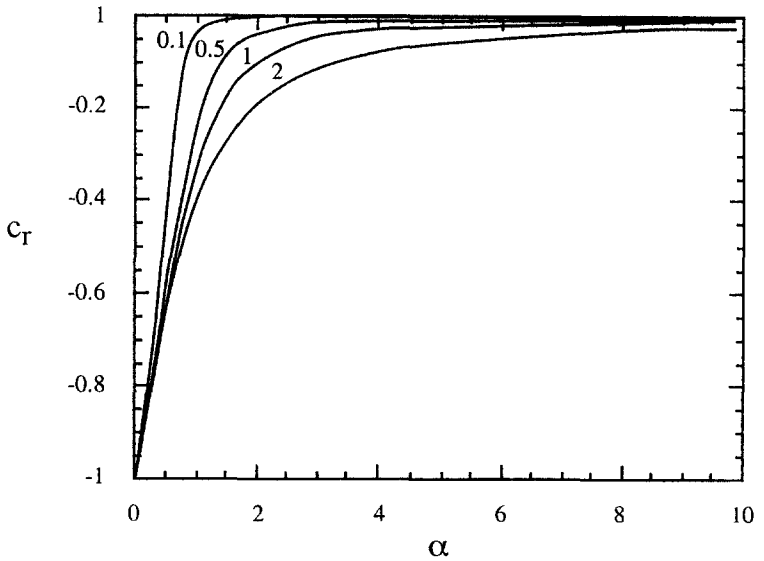

Fig. 3. – Wave speeds for the sinuous mode for a purely viscous jet. Re = 0.1, 0.5, 1.0, 2.0. The numbers above each curve are the corresponding Reynolds numbers.

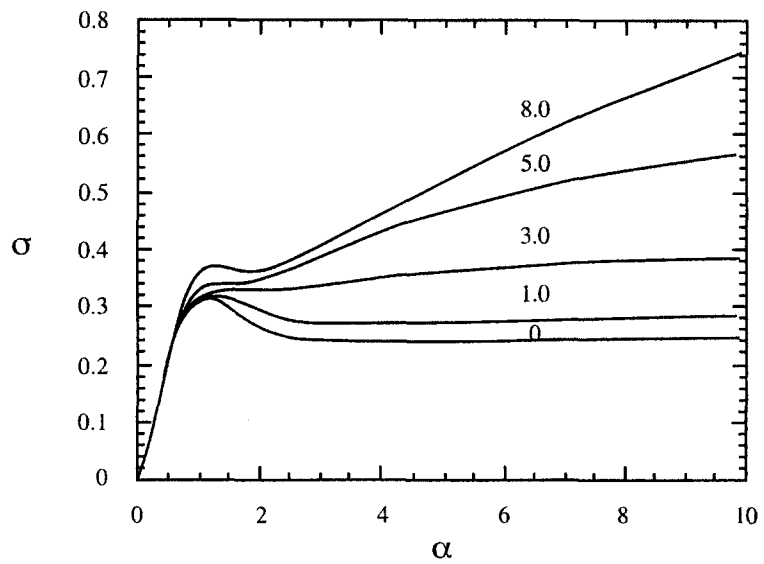

Fig. 4. – Growth rates for the sinuous mode for Re = 0.5, $\varepsilon = 0$, $E = 0, 1.0, 2.0, 3.0, 5.0, 8.0$ ($0 \leq \chi \leq 2$). The numerical values above each curve are the corresponding elasticity numbers E.

rate, as shown in Figure 6, increases with the elasticity parameter E for $0 \leq E < 2.0$, which corresponds to the viscous mode, modified by elasticity. When $E = 2$, then $\chi = 2$, and the growth rate becomes unbounded as $\alpha \to \infty$. As the elasticity is increased from $E = 2$ to 2.4, and then to 3.0, however, the growth rate is reduced. When the elasticity is increased further to $E = 3.1$ and beyond, the growth rate starts to increase again. For $2 < \chi \leq 3.2135$, the unstable mode is an elastic mode, and the growth rate levels off to a constant as $\alpha \to \infty$. All these unstable elastic modes have finite wave speeds when $\alpha \to \infty$, as compared to zero for the viscous mode (*see* Figure 7). Elasticity reduces the wave speed. The values $E = 2.0$, 3.2135 correspond to $\chi = 2$, 3.2135, and the wave speeds approach 0 and -0.354137, respectively (*see* equations (5.13) and (5.14), and

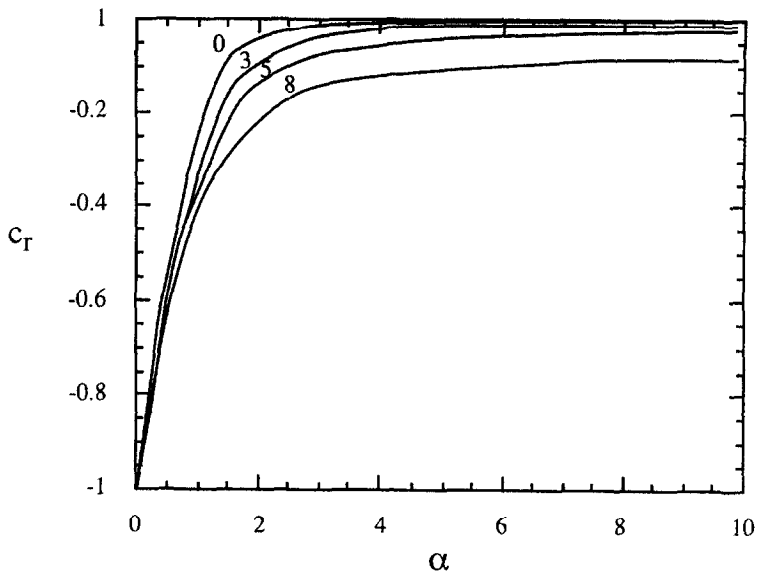

Fig. 5. – Wave speeds for the sinuous mode for Re = 0.5, $\varepsilon = 0$, $E = 0, 3.0, 5.0, 8.0$ $(0 \leq \chi \leq 2)$. The corresponding elasticity numbers are marked above each curve.

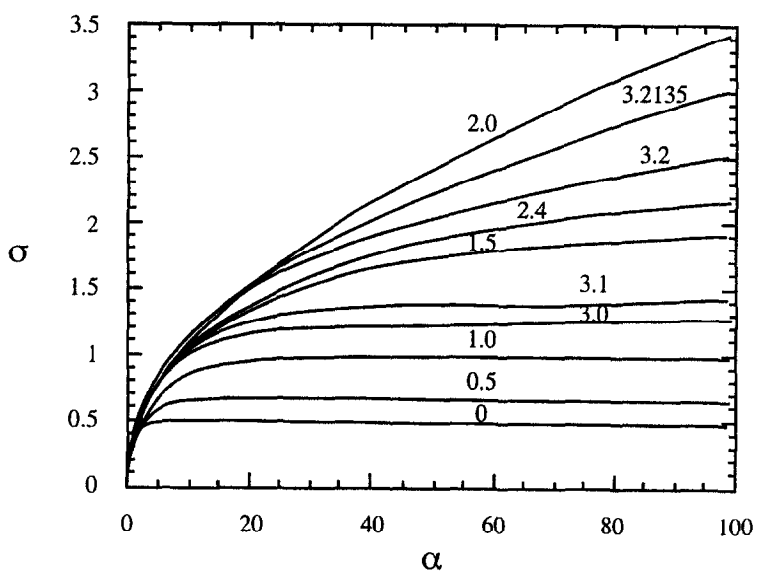

Fig. 6. – Growth rates for the sinuous mode for Re = 1.0, $\varepsilon = 0$, $E = 0, 0.5, 1.0, 1.5, 2.0, 2.4, 3.0, 3.1, 3.2, 3.2135$. $(0 \leq \chi \leq 3.2135)$. Elasticity number is indicated above each curve.

the statements thereafter). (The reader is reminded that the analysis here is in a reference frame in which the jet has no mean velocity, and statements about the increase or decrease of wave speeds refer to the algebraic (signed) wave velocities in that frame. In the laboratory frame (surroundings of the jet at rest) the situation is different. Wave speeds approach the jet velocity (from below) as $\alpha \to \infty$, but elasticity still reduces the wave speeds at a given α.)

Computations for $\chi > 3.2135$ have been carried out for Re = 15, 25, 100, 200. These results are similar, and all indicate that elasticity increases the growth rate, and reduces the wave speed. The results for Re = 25, which is typical for a plane jet, are presented in Figures 8 and 9.

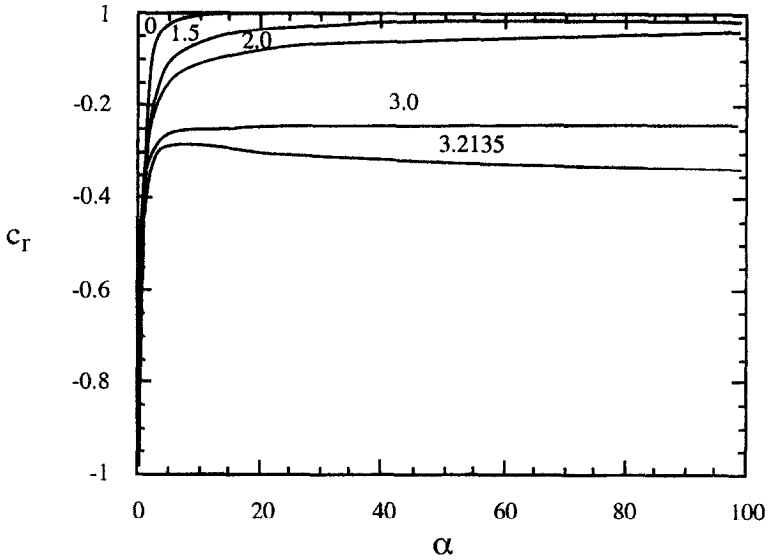

Fig. 7. – Wave speeds for the sinuous mode for Re = 1.0, $\varepsilon = 0$, $E = 0$, 1.5, 2.0, 3.0, 3.2135. ($0 \leq \chi \leq 3.2135$). The modified viscous mode ($E = 1.5$) and the elastic mode ($E = 3.0$) have distinct wave speed limits for very short waves.

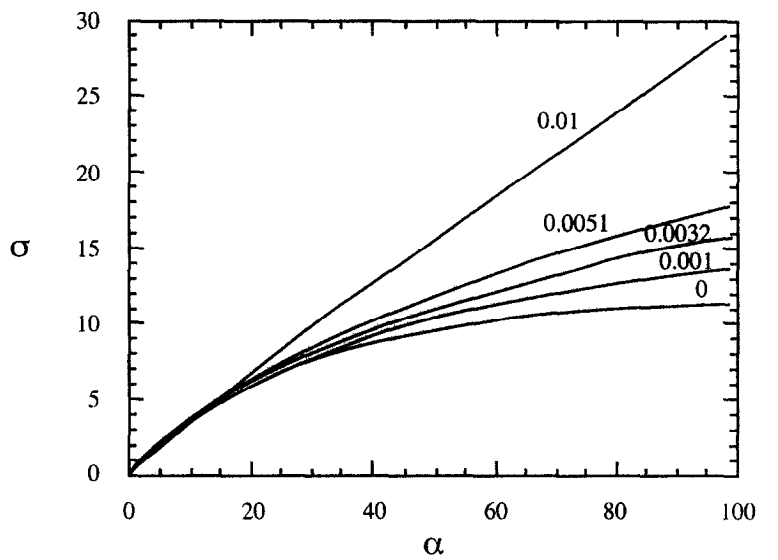

Fig. 8. – Growth rates for the sinuous mode for Re = 25, $\varepsilon = 0$, $E = 0$, 0.001, 0.0032, 0.0051, 0.01. The elasticity number E is marked above each curve.

Computations have also been carried out for $\varepsilon \neq 0$. A non-zero ε has the effect of reducing the growth rate and increasing the wave speed. For any non-zero ε, both the growth rate and the wave speed fall between the purely viscous case ($E = 0$) and the highly elastic case ($\varepsilon = 0$), and the jet behaves more and more like a purely viscous jet as the value of ε is increased. This is analogous to the situation in non-Newtonian fluid mechanics when the fluid is modeled by an Oldroyd-B equation, whose linearization gives our equation (3.5). In particular, the growth rate for short waves is forced to be bounded for all wavenumbers when $\varepsilon \neq 0$. An example is given for Re = 25 in Figures 10 and 11.

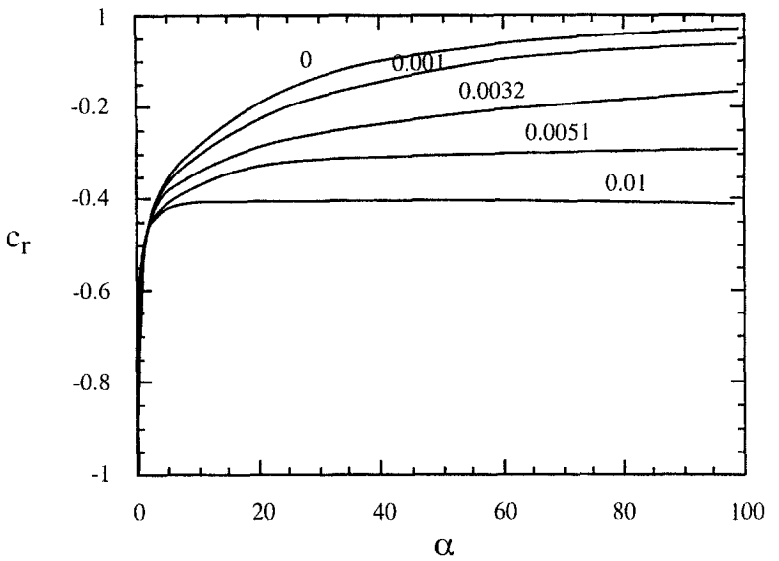

Fig. 9. – Wave speeds for the sinuous mode for Re = 25, $\varepsilon = 0$, $E = 0.001, 0.0032, 0.0051, 0.01$. The elasticity number E is indicated above each curve. Different limits are approached by the viscous mode and the elastic mode for short waves.

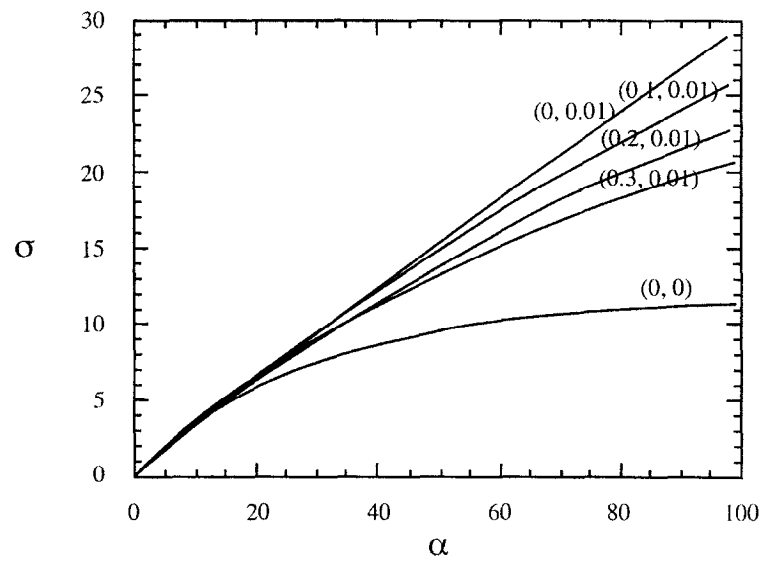

Fig. 10. – Growth rates for Re = 25. The values for (ε, E) are indicated above each curve. Increasing ε reduces the growth rate and makes the jet ever closer to a purely viscous jet with $(\varepsilon, E) = (0, 0)$.

8. The varicose mode

The dispersion relation for the varicose mode is given by equation (4.11), and we shall only discuss the case with $\varepsilon \neq 0$. In the long wave limit $\alpha \to 0$, the eigenvalue c takes the following asymptotic form:

$$c = \pm i\alpha^{1/2} - \alpha\left(1 + i\frac{2}{\mathrm{Re}}\right) \pm \alpha^{3/2}\left(\frac{2\mathrm{Re} + i(2 - \mathrm{Re}^2)}{\mathrm{Re}^2}\right) + O(\alpha^2). \tag{8.1}$$

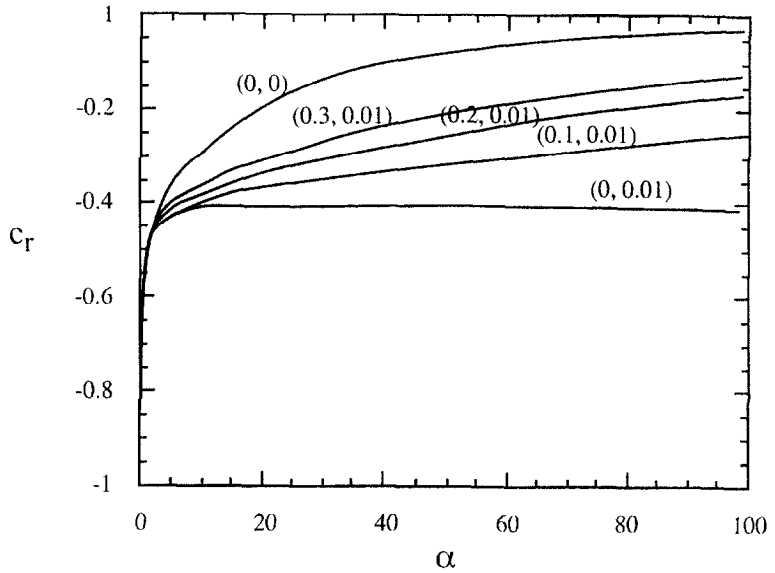

Fig. 11. – Wave speeds for Re = 25. The values for (ε, E) are indicated above each curve. Increasing ε increases the wave speed and makes the jet ever closer to a purely viscous jet $(\varepsilon, E) = (0, 0)$.

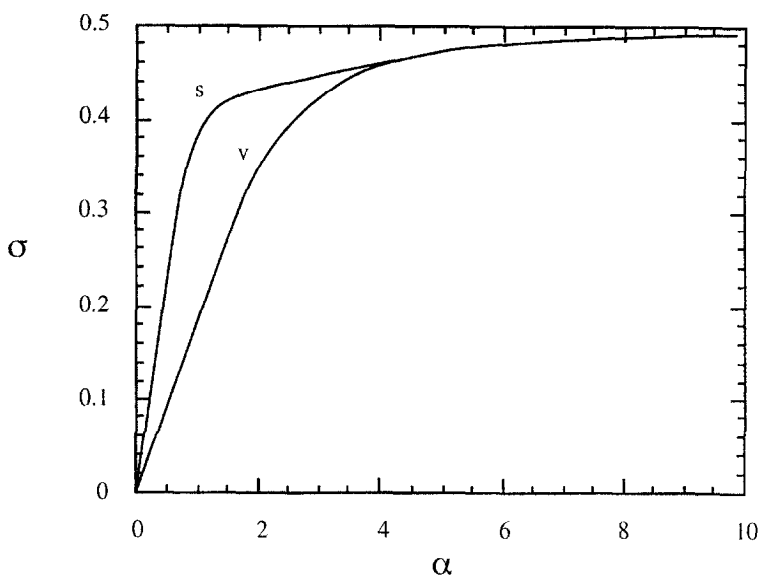

Fig. 12. – Growth rates for a purely viscous jet at Re = 1.0. "s" stands for the sinuous mode and "v" stands for the varicose mode.

For long waves, the growth rate for the varicose mode is $\alpha^{3/2}\left(1 - \alpha^{1/2}\frac{2}{\mathrm{Re}} + \alpha\frac{2 - \mathrm{Re}^2}{\mathrm{Re}^2}\right) + O(\alpha^2)$, as compared to $\alpha^{3/2} + O(\alpha^2)$ for the sinuous mode. Thus, the varicose mode always has a smaller growth rate than the sinuous mode in the long wave limit, and the difference between the growth rates of these two modes is larger for small Reynolds numbers. Furthermore, to leading order for very long waves, the varicose mode is stationary (zero wave speed), while the sinuous wave is convected with the external velocity (wave speed equals -1), in both cases as for a purely inviscid inelastic jet flow. In the laboratory frame, the varicose mode propagates downstream at the jet velocity, while the sinuous mode remains almost at rest.

In the short wave limit, $\alpha \to \infty$, and $\varepsilon \neq 0$, the varicose mode has the same asymptotic form as the sinuous mode, given by equation (6.1b). To compare the varicose and the sinuous modes for arbitrary wavenumbers, we have computed the growth rates and the wave speeds for both modes for the set of parameters $\mathrm{Re} = 1$, 15, $\varepsilon = 0$, $E = 0$, which correspond to a purely viscous jet. These results are presented in Figures 12-15. For any wavenumber, the growth rate for the varicose mode is always smaller than that for the sinuous mode, and the difference in the growth rates for these two modes increases as the Reynolds number is decreased (Figures 12 and 14). These two modes have very distinct wave speeds, particularly for longer waves. The sinuous mode is essentially stationary and the varicose mode propagates with the jet (Figures 13 and 15). In the short wave limits, these two modes are indistinguishable, as the two bounding surfaces separating turbulent and non-turbulent fluids become independent of each other. Elasticity of the jet is found to have effects on the instability characteristics for the varicose mode similar to those for the sinuous mode discussed earlier. The sinuous mode always has a larger growth rate than the varicose mode, whether the jet is elastic or not. Even for the case of an elastic jet, the dominance of the sinuous mode instability cannot be attributed to the "buckling" mechanism because the basic state considered here is not sheared.

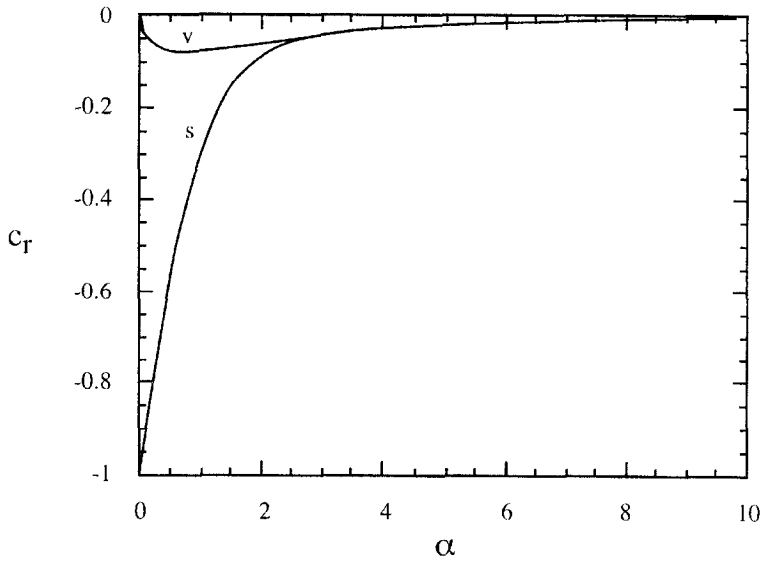

Fig. 13. – Wave speeds for a purely viscous jet at $\mathrm{Re} = 1.0$. "s" stands for the sinuous mode and "v" stands for the varicose mode.

9. Summary and conclusion

This study is aimed at understanding of the generation and propagation of large scale organized waves in a turbulent jet from the point of view of viscoelastic modeling of the perturbation Reynolds stress. The foundation for the viscoelastic modeling of the incremental Reynolds stress caused by the imposition of a large scale perturbation for the simplified problem considered here was laid by Crow (1968) more than two decades ago for fine-grained isotropic turbulence. The problem studied here is the viscoelastic generalization of the turbulent jet stability problem analyzed by Townsend (1966) using alternate purely viscous and purely elastic response assumptions. Townsend found that for very short waves, while the purely viscous jet suffers an instability, the purely elastic jet is stable at low jet speed. Only when the jet speed exceeds a critical value, which is proportional to the square-root of the rigidity, does the purely elastic jet becomes unstable to short waves. The present study shows, however, that for a viscoelastic jet (or when the perturbation Reynolds stress is modeled viscoelastically), which includes both the purely viscous and the purely elastic cases as extreme limits, the short waves are always unstable, though with at most finite growth rates which are always smaller than those for the

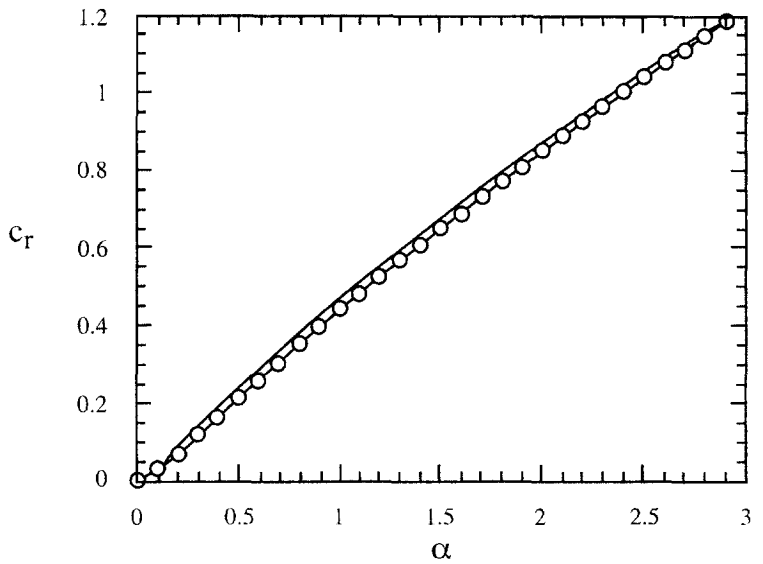

Fig. 14. – Growth rates for a purely viscous jet at Re = 15.
The curve marked with circles is for the varicose mode and the solid line for the sinuous mode.

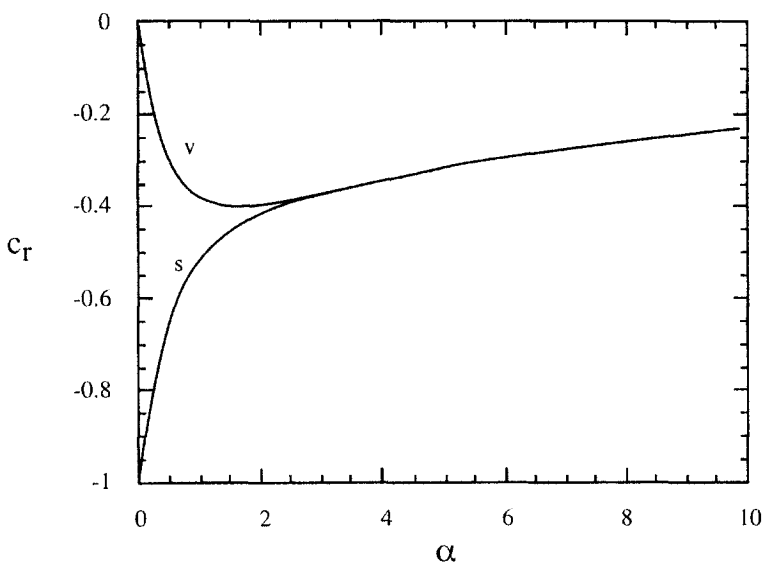

Fig. 15. – Wave speeds for a purely viscous jet at Re = 15. "*s*" stands for the sinuous mode and "*v*" stands for the varicose mode.

classical Kelvin-Helmholtz instability of an inviscid jet, but larger than those for the Hooper-Boyd instability of a viscous jet with continuous velocity profile. These instabilities can never be stabilized, at least in the linear regime. Moreover, the anti-symmetric sinuous mode grows faster than the symmetric varicose mode, even when the base flow has a uniform velocity profile. Naturally the predictions provided by this study cover only the frequency range for which the wavelength exceeds the (small) scale of the fine-grained turbulence. And of course that is the same condition as the one that allows the shear layer to be treated as a discontinuity.

The results obtained from our analysis also applies to a viscoelastic jet modeled by the Oldroyd-B constitutive equation. Elasticity is found to enhance instability and reduce wave speed. This may have implications to many industrial applications involving viscoelastic fluids.

10. Further development

The instabilities found in this study are essentially of Kelvin-Helmholtz type due to the vortex sheet model used for the base velocity profile. In reality, the turbulence is produced by the shearing of the base state, and there are never velocity discontinuities at the surfaces bounding the turbulent and non-turbulent fluids. The viscoelastic constitutive equation for the incremental Reynolds stress induced by a large scale perturbation to the base state needs now to be generalized to turbulent shear flows maintained by a non-zero mean shear. Such a generalization has been suggested by both Crow (1968) and Lumley (1970). In particular, Lumley made this statement to conclude his paper: "In particular, it may be useful to predict the small changes in Reynolds stress caused by the imposition of secondary motions (big eddies) on the basic mean motion. As such, it has the desirable property of displaying viscoelastic behavior as Townsend (1966) has concluded is necessary." The present paper is just the first step for such an analysis. The results obtained here show that the presence of the Reynolds stress relaxation time θ_1 can introduce new instability modes which are purely elastic in nature and are completely absent in models without stress-relaxation. For a sheared turbulent jet, there exists another elastic instability mechanism, which is due to the action of the Reynolds-stress anisotropy of the basic state on the perturbation field. The anisotropy of the Reynolds stress of the basic state creates an equivalent compression along the mean streamlines of the basic state. The mean streamlines which are under compression can then become unstable under large-scale perturbations. It is apparent that such an analysis for more realistic jets, to which the authors will next turn their attention, should add to the understanding of the organized wave motions in a turbulent jet.

APPENDIX

Coefficients $p_i(1 \geq i \geq 7)$ of the dispersion relation (4.8)

$$
\begin{aligned}
p_1 &= 2c\beta\mathrm{Re}(\beta^2 - \alpha^2)(1+c)^2(3i\alpha^2 Q - i\beta^2 Q + \alpha c\mathrm{Re}),\\
p_2 &= c\mathrm{Re}(\alpha^4 - \beta^4)(1+c)^2(2i\alpha Q + c\mathrm{Re}),\\
p_3 &= -\mathrm{Re}^2[2c^4(\alpha^2+\beta^2)^2 + \alpha^2 - \beta^2)^2(1+2c)(2c^2+2c+1)\\
&\qquad -Q4i\alpha c^3\mathrm{Re}(\alpha^4 + 8\alpha^2\beta^2 + \beta^4) + Q^2 4c^2(\alpha^6 + 11\alpha^4\beta^2 - 5\alpha^2\beta^4 + \beta^6)],\\
p_4 &= 2\beta c^2(\alpha^2+\beta^2)(2i\alpha Q + c\mathrm{Re})(3i\alpha^2 Q - i\beta^2 Q + \alpha c\mathrm{Re}),\\
p_5 &= 2\beta c^2(\alpha^2+\beta^2)(2i\alpha Q + c\mathrm{Re})(3i\alpha^2 Q - i\beta^2 Q + \alpha c\mathrm{Re}),\\
p_6 &= 2c\beta\mathrm{Re}(\beta^2 - \alpha^2)(1+c)^2(3i\alpha^2 Q - i\beta^2 Q + \alpha c\mathrm{Re}),\\
p_7 &= c\mathrm{Re}(\alpha^4 - \beta^4)(1+c)^2(2i\alpha Q + c\mathrm{Re}).
\end{aligned}
$$

Acknowledgment. – Chen's work is partially supported by the National Science Foundation grant CTS-9157063.

REFERENCES

AITKEN L. S. and WILSON S. D. R. 1993, Rayleigh-Taylor instability in elastic liquids, *J. Non-Newt. Fluid Mech.*, **49**, 13–22.

AZAIEZ J. and HOMSY G. M. 1994, Linear stability of free shear flow of viscoelastic liquids, *J. Fluid Mech.*, **268**, 37–69.

CROW S. C., 1968, Viscoelastic properties of fine-grained incompressible turbulence, *J. Fluid Mech.*, **33**, 1–20.

FRISCH U., SHE Z. S. and THUAL O., 1986, Viscoelastic behavior of cellular solutions to the Kuramoto-Sivashinsky model, *J. Fluid Mech.*, **168**, 221–240.

HOOPER A. P. and BOYD W. G., 1983, Shear flow instability at the interface between two viscous fluids, *J. Fluid Mech.*, **128**, 507–528.

JOSEPH D. D., 1990, Fluid Dynamics of Viscoelastic Liquids, Springer-Verlag, New York.

KASSINOS S. C. and REYNOLDS W. C. 1994, A structure-based model for the rapid distortion of homogeneous turbulence. Stanford University Report, TF-61.

LIEPMANN H. W., 1961, Free turbulent flows. Mécanique de la Turbulence, 211–226, Paris, CNRS.

LUMLEY J. L., 1970, Toward a turbulent constitutive relation, *J. Fluid Mech.*, **41**, 413–434.

MOFFATT H. K. 1965, The Interaction of Turbulence with Rapid Uniform Shear. SUDAER Rep. no. 242, Stanford University.

MOFFATT H. K., 1967, The interaction of turbulence with strong wind shear. In Atmospheric Turbulence and Radio Wave Propagation (Ed. YAGLOM A. M. and TATARSKY V. I.), 139–154. Publishing House 'Nauka', Moscow, 1967.

RALLISON J. M. and HINCH E. J. 1995, Instability of a high-speed submerged elastic jet, *J. Fluid Mech.*, **288**, 311–324.

REYNOLDS W. C., 1972, Large-scale instabilities of turbulent wakes, *J. Fluid Mech.*, **54**, 481–488.

RIVLIN R. S. 1957, The relation between the flow of non-Newtonian fluids and turbulent Newtonian fluids, *Q. Appl. Math.*, **15**, 212–215.

SAFFMAN P. G., 1977, Results of a two-equation model for turbulent flows and development of a relaxation stress model for application to straining and rotating flows. Proc. Project SQUID Workshop on Turbulence in Internal Flows (MURTHY S., ed.), 191–231, Hemisphere.

SHE Z. S., FRISCH U. and THUAL O., 1985, Homogenization and visco-elasticity of turbulence. In Macroscopic Modeling of Turbulent Flows, ed. FRISCH U., KELLER J. B., PAPANICOLAOU G. and PIRONNEAU O., Lecture Notes in Physics, **230**, 1–12.

SPEZIALE C. G. and XU X. H., 1995, Towards the development of second-order closure models for non-equilibrium turbulent flows, Tenth Symposium on Turbulent Shear Flows, Penn State University, August 1995.

TENNEKES H. and LUMLEY J. L., 1972, A First Course in Turbulence. MIT Press.

TOWNSEND A. A., 1966, The mechanism of entrainment in free turbulent flows, *J. Fluid Mech.*, **26**, 689–715.

WILSON S. D. R., 1990, The Taylor-Saffman problem for a non-Newtonian liquid, *J. Fluid Mech.*, **220**, 413–425.

(Received 21 August 1997;
revised 19 February 1998;
accepted 13 March 1998.)